

Development of a New Titanium Powder Sintering Process with Deoxidation Reaction Using Yttrium Metal

Akihiro Iizuka^{1,2,*1}, Takanari Ouchi^{1,*2} and Toru H. Okabe¹

¹Institute of Industrial Science, The University of Tokyo, Tokyo 153-8505, Japan

²Department of Materials Engineering Graduate School of Engineering, The University of Tokyo, Tokyo 113-8656, Japan

Oxygen (O) contamination in titanium (Ti) is difficult to control using conventional Ti powder-metallurgy technologies, owing to the strong affinity between Ti and O. In this study, we developed a new sintering process that can remove O from Ti by placing Ti green and yttrium (Y) in molten salt. This study demonstrates that the O concentration in Ti can be reliably controlled in the range of 200–2000 ppm O by varying a_Y in the Y/Y₂O₃ equilibrium at 1300 K in NaCl–KCl (*l*), such that the sintering reaction of Ti powder simultaneously proceeds. Furthermore, it is also shown that the O concentration in Ti can be reduced to 30–60 ppm O in YCl₃ (*l*) in the sintering process, when the Y/YOCl/YCl₃ equilibrium is employed. This study demonstrates the feasibility of a new sintering process that can control the O concentration in Ti to approximately 30–2000 ppm O. The process ensures economical rationality because the cost of Y metal is negligibly small in recent years. By developing this process, inexpensive high-O-concentration Ti powder can be applied for fabricating the desired low-O-concentration Ti products. [doi:10.2320/matertrans.MT-M2019340]

(Received November 19, 2019; Accepted January 28, 2020; Published March 25, 2020)

Keywords: low-oxygen titanium, rare earth metals, sintering, molten salt

1. Introduction

Titanium (Ti) and Ti-alloy (Ti–6 mass% Al–4 mass% V, etc.) have desirable properties such as low weight, high strength, corrosion resistance, and biocompatibility.^{1–4} Additionally, Ti has an abundant natural resource, and Ti material is expected to become a major industrial metal such as steel and aluminum.^{5,6} However, the current production costs of Ti products are much higher than those made from common metals so that the use of Ti is limited to high-value-added products for specific applications, such as aircraft parts.⁷ The high production cost of Ti products is caused by inefficient, specialized, and high-cost techniques to control the purity of Ti in smelting and machining processes. This is mainly because Ti has an extremely strong affinity for oxygen (O) at high temperatures.⁷

Powder metallurgy of Ti (PM-Ti) is suitable for producing Ti products, because it can decrease the number of high-temperature processes in machining (a near-net-shaped process). In recent years, PM-Ti technologies (e.g., 3D-printing) fields have advanced rapidly worldwide. Moreover, many new smelting methods for Ti were developed to reduce smelting costs and designed to produce Ti powder.^{8–11} PM-Ti has attracted much attention as a critical technology to enable the widespread use of Ti in our society.

With conventional PM-Ti technologies, the increase of the O concentration in Ti during the sintering process is unavoidable owing to the strong affinity between Ti and O.¹² As the O concentration in Ti increases, the tensile strength also increases because of the solid solution strengthening effect, but the ductility of Ti deteriorates significantly.^{13–17} During the manufacture of low-O-concentration Ti products, expensive pure Ti powder with low-O-concentrations (e.g., 200–400 USD·kg⁻¹)^{18,19} is required as starting material, resulting in high production costs.

Considering the current trade-offs between strength and ductility, it would certainly be beneficial to develop a new deoxidation technology to control the O concentration in Ti to 100–2000 mass ppm O. The deoxidation technology will establish a novel sintering process that can produce Ti products with the desired O concentration starting from an inexpensive high-O-concentration Ti powder.

Until recently, a variety of methods that can produce sintered Ti with low-O-concentrations have been proposed and developed (Table 1).^{20–34} Generally, the sintering process of Ti is conducted in an inert-gas atmosphere or a vacuum. However, as shown in Table 1, the O concentration in Ti is inevitably increased in inert-gas and vacuum states during the sintering process. This occurs, because the partial pressure of O₂ (i.e., O₂ potential), p_{O_2} , must be extremely low to directly remove O from Ti, owing to the strong affinity between Ti and O. Based on equilibrium theory, the relationship between the O concentration in β -Ti ($[O]_{Ti}$ (mass%)) and p_{O_2} is expressed as follows:³⁵

$$1/2 O_2 (g) = O (1 \text{ mass\%, in } \beta\text{-Ti}) \quad (1)$$

$$\Delta G^\circ_{1,Ti} = -2.303 RT \log(f_O \cdot [O]_{Ti}/p_{O_2}^{1/2}) \quad (2)$$

$$\Delta G^\circ_{1,Ti} = -583000 + 88.5T \text{ (J) [1173–1373 K]} \quad (3)$$

where O dissolved in Ti is expressed relative to the 1 mass% standard state; $\Delta G^\circ_{1,Ti}$ is the standard Gibbs energy of the O dissolution in Ti; R is the gas constant; T is the absolute temperature; and f_O is the Henrian activity coefficient for O dissolved in Ti. Given that the O dissolved in Ti obeys Henry's law, the value of f_O is defined to be unity.

For example, when 1 mass% O (10000 ppm O) is dissolved in β -Ti at 1300 K, p_{O_2} is determined to be as low as 2.5×10^{-38} atm (2.5×10^{-33} Pa). At such an extremely low O₂ potential, direct removal of O from Ti during the sintering process is impossible in an inert gas or vacuum state. Therefore, Ti powder with low-O-concentration is greatly needed for conventional PM-Ti technologies. However, low-O-concentration Ti powder is expensive, because it is difficult to produce with high-purity using conventional technologies.

*1Graduate Student, The University of Tokyo

*2Corresponding author, E-mail: t-ouchi@iis.u-tokyo.ac.jp

Table 1 Previous studies of the production of sintered Ti at low-oxygen concentrations.

Author, year	Method	Initial oxygen concentration of Ti powder, $C_{o,initial}$ (ppm O)	Oxygen concentration of sintered Ti, $C_{o,sintered}$ (ppm O)
S. Abkowitz <i>et al.</i> , 1971 ²⁰⁾	Unknown		415
K. Majima, <i>et al.</i> , 1984 ²¹⁾	Sintered under vacuum	1500	2000
K. Majima, <i>et al.</i> , 1984 ²¹⁾	Sintering with Ca vapor	1500	1960
P.K. Tripathy, <i>et al.</i> , 2007 ²²⁾	Electrochemical method in $\text{CaCl}_2(l)$	TiO_2	< 1500
L. Strezov, <i>et al.</i> , 2007 ²³⁾	Electrochemical method in $\text{CaCl}_2(l)$	TiO_2	< 500
J.C. Choi <i>et al.</i> , 2009 ²⁴⁾	Sintering Ti powder with Ca under vacuum		7100
A.T. Sidambe, <i>et al.</i> , 2014 ²⁵⁾	Sintering in Ar	1430	1700
S.D. Luo, <i>et al.</i> , 2013 ²⁶⁾	Microwave sintering with Ti sponge		2100
E. Carreño-Morelli, <i>et al.</i> , 2014 ²⁷⁾	Sintering TiH_2 powder	TiH_2	3000
J.M. Oh, <i>et al.</i> , 2016 ²⁸⁾	Sintering with Ca and CaCl_2 vapor	2000	3000–3100
Z.Z. Fang, <i>et al.</i> , 2017 ²⁹⁾	“Partial sintering” in $\text{CaCl}_2(l)$		< 1000
The aim of this study, 2019	Utilizing $\text{Y}/\text{Y}_2\text{O}_3$ equilibrium		200–2000
	Utilizing $\text{Y}/\text{YOCl}/\text{YCl}_3$ equilibrium		30–60

Based on this background, many researchers have focused on using deoxidizing agents in PM-Ti. In particular, calcium (Ca) metal is well known for its strong deoxidizing capability and its high vapor pressure. For example, in 1984, Majima *et al.* reported a sintering method for Ti powder in Ca vapor, but the O concentration in Ti increased during the process.²¹⁾ Until recently, some researchers (e.g., Choi *et al.* and Oh *et al.*) had reported sintering methods for Ti in Ca vapor.^{24,28)} Nevertheless, the sintering methods of Ti using Ca vapor are not widely used at an industrial scale, partly because it is challenging to efficiently remove the by-products of the deoxidation reaction (e.g., CaO (*s*)) from inside the sintered Ti body.

In molten salts, such as $\text{CaCl}_2(l)$, which is stable at extremely low O_2 potential, the solubility of the oxide ion (O^{2-}) is high. Thermochemical and electrochemical deoxidation processes in molten salts are widely known as efficient techniques to remove O from Ti. Ca metal is widely known as an efficient deoxidizing agent for Ti in CaCl_2 , and many researchers have reported that the sintering reaction of Ti powders occurred in molten salt.^{28,36–43)} Additionally, researchers have produced sintered Ti from TiO_2 powder using an electrochemical process with molten salt. In 2007, Tripathy *et al.* produced sintered Ti with 1500 ppm O or less by applying a voltage between a TiO_2 cathode and a carbon

anode in CaCl_2 (Fray–Farthing–Chen Cambridge method, FFC method).^{22,44)} In the same year, Strezov *et al.*²³⁾ reported in a patent that they had produced sintered Ti with 500 ppm O or less using the FFC method. More recently, Hu *et al.* produced golf-club-sized sintered Ti using the FFC method.^{30,31)}

To the best of our knowledge, there has been no report about producing sintered Ti with reliably lower than 400 ppm O, or of precisely controlling the O concentration in Ti in the range of 100–2000 ppm O. In conventional PM-Ti technologies, O concentrations in Ti increase during the sintering process and expensive Ti powder with low-O concentration is necessary to produce reliable Ti products. To solve this problem for PM-Ti, we focused on developing a new sintering process that controls the O concentration in Ti using the deoxidation techniques of pyrometallurgy.

In the past, the amounts of rare-earth (RE) metals production were small, and it was not economical to use RE metals for the deoxidation of Ti on an industrial scale. However, the demand for RE magnets, especially Nd–Fe–B magnets doped with Dy, has rapidly increased in recent years.⁴⁵⁾ Some RE metals, including Y, La, Ce, and Ho are produced as by-products of Nd and Dy. Industrially, the applications of these RE metals are limited and their demands are not expected to increase. Therefore, there will be a chronic oversupply of these RE metals in the future. Thus, the use of Y, La, Ce, and Ho metals for new deoxidation technology in PM-Ti ensures efficient utilization of natural resources and can be justified economically.

In PM-Ti fields, some researchers have reported that the mechanical properties of sintered Ti could be improved with small additions of RE compounds (RE oxides, RE hydrides, RE borides, etc.).^{46–48)} Especially, the mechanical strengthening effect due to oxide particle distribution by internal oxidation of RE elements is actively studied.

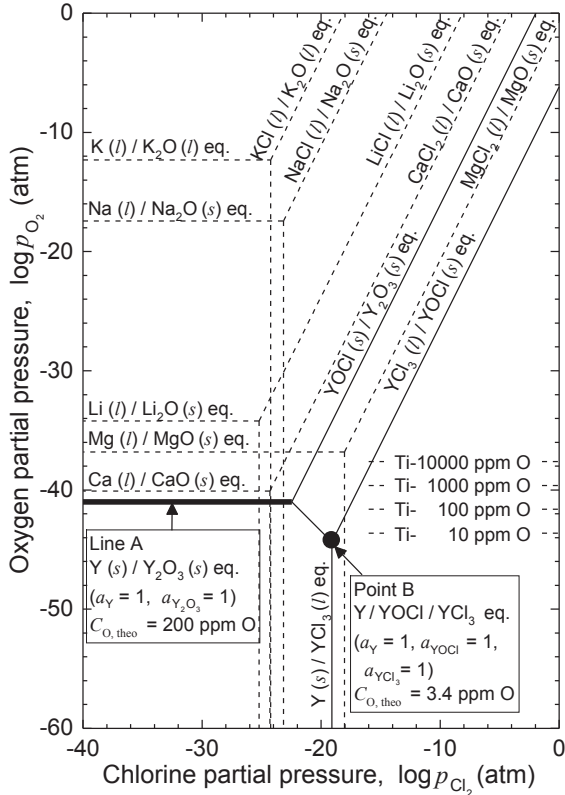
In contrast, we focused on the deoxidation of Ti by dissolving O in molten salt using RE metals. The deoxidation limits in the $\text{RE}/\text{RE}_2\text{O}_3$ equilibrium for bulk Ti have been experimentally demonstrated.^{49–53)} Specifically, Y is considered to have the strongest deoxidizing capability in the $\text{RE}/\text{RE}_2\text{O}_3$ equilibrium in all rare earth metals. For example, when $a_Y = 1$ and $a_{\text{Y}_2\text{O}_3} = 1$ at 1300 K, the O concentration in bulk Ti decreases to approximately 100–200 ppm O in the $\text{Y}/\text{Y}_2\text{O}_3$ equilibrium. Just recently, we experimentally demonstrated that the O concentration in Ti could be decreased to 30–60 ppm O in the $\text{Y}/\text{YOCl}/\text{YCl}_3$ equilibrium at 1300 K.⁵³⁾ However, there has been no research on the behavior of Ti powder at such an extremely low O_2 potential ($p_{\text{O}_2} < 2.5 \times 10^{-42}$ atm at 1300 K, O concentration in Ti < 100 ppm O).

In this study, we developed a new sintering process that can remove O from Ti using Y metal as the deoxidizing agent in molten salt. Our goal is to demonstrate a new sintering process in which the O concentration in Ti can be controlled within the range of approximately 30–2000 ppm O (Table 1).

2. Thermodynamic Consideration

To design a new deoxidation method using molten salt, we determined the deoxidation reaction and the molten salt

M-Cl-O system at 1300 K (M = Li, Na, K, Ca, Mg, Y)

Fig. 1 Phase stability diagram for the M-Cl-O system (M = Li, Na, K, Mg, Ca and Y) at 1300 K.^{15,54,55)}

suitable to control the O concentration in Ti using a thermodynamic consideration. We set the experimental temperature to 1300 K, because this temperature is experimentally known to facilitate the deoxidation of Ti in molten salt.

In the Y-O-Cl system at 1300 K, $Y_2O_3(s)$, $YOCl(s)$, and $YCl_3(l)$ are reported as stable compounds. Figure 1 shows a phase stability diagram produced from a plot of the partial pressure of Cl_2 , p_{Cl_2} , vs. the partial pressure of O_2 , p_{O_2} , for the M-O-Cl system (M = Li, Na, K, Ca, Mg, Y) at 1300 K. Table 2 shows the thermodynamic data used to draw Fig. 1.^{35,54,55)} The relationship between the O concentration in Ti and p_{O_2} based on equilibrium theory, is also expressed in Fig. 1 using eqs. (1)–(3).

As shown in Fig. 1, LiCl, NaCl, KCl, and $CaCl_2$ have regions coexisting with the Y/ Y_2O_3 equilibrium (Line A) and the Y/ $YOCl$ / YCl_3 equilibrium (Point B). Thus, in molten LiCl, NaCl, KCl, and $CaCl_2$, Y metal is stable and the following deoxidation reactions proceed at 1300 K. In $MgCl_2$, Y metal is unstable.



$$\Delta G_{r, \text{deox [4]}}^\circ = 1/3 \Delta G_{f, Y_2O_3}^\circ - \Delta G_{f, Ti}^\circ \quad (5)$$

$$[O]_{Ti [4]} = (a_{Y_2O_3}^{1/3} / a_Y^{2/3}) \exp(\Delta G_{r, \text{deox [4]}}^\circ / RT) \quad (6)$$

$$C_{O, \text{theo [4]}} = 200 (a_{Y_2O_3}^{1/3} / a_Y^{2/3}) \text{ (mass ppm O)} \quad (7)$$



$$\Delta G_{r, \text{deox [8]}}^\circ = \Delta G_{f, YOCl}^\circ - 1/3 \Delta G_{f, YCl_3}^\circ - \Delta G_{f, Ti}^\circ \quad (9)$$

Table 2 Standard Gibbs free energy of formation at 1300 K used in Fig. 1 drawing.

Species, <i>i</i>	Standard Gibbs energy of formation, $\Delta G_{f,i}^\circ$ /kJ·mol ⁻¹ at 1300 K	Ref.
O (1 mass %, in β -Ti)	- 468	15
LiCl (l)	- 314	54
Li ₂ O (s)	- 426	54
NaCl (l)	- 288	54
Na ₂ O (s)	- 216	54
KCl (l)	- 302	54
K ₂ O (l)	- 153	54
MgCl ₂ (l)	- 449	54
MgO (s)	- 458	54
CaCl ₂ (l)	- 605	54
CaO (s)	- 499	54
Y ₂ O ₃ (s)	- 1530	54
YCl ₃ (l)	- 713	54
YOCl (s)	- 790	55

$$[O]_{Ti [8]} = (a_{YOCl} / (a_Y^{2/3} \cdot a_{YCl_3}^{1/3})) \exp(\Delta G_{r, \text{deox [8]}}^\circ / RT) \quad (10)$$

$$C_{O, \text{theo [8]}} = 3.4 (a_{YOCl} / (a_Y^{2/3} \cdot a_{YCl_3}^{1/3})) \text{ (mass ppm O)} \quad (11)$$

where $\Delta G_{f,i}^\circ$ is the standard Gibbs free energy of formation for each compound; a_i is the activity of each chemical species; and $C_{O, \text{theo}}$ is the O concentration in Ti (mass ppm O).

Conversely, when Y metal is placed in molten $MgCl_2$, the following displacement reaction occurs:



As long as $MgCl_2$ exists in the system, Y metal induces the displacement reaction with $MgCl_2$ (eq. (12)). In this study, $MgCl_2$ was excluded from the flux candidates for the sintering process in order to use Y metal as the deoxidizing agent.

There is a possibility that the sintering Ti samples were contaminated by Y and other elements. For example, Y has a very small solubility in Ti (approximately 0.2 mol% at 1300 K) based on available thermodynamic data in the literature.⁵⁶⁾ This study is a proof-of-concept of the new sintering process with deoxidation, and the contamination of such elements should be investigated in detail as future works.

Figure 2 shows the relationship between $[O]_{Ti}$ and a_Y in the Y/ Y_2O_3 and Y/ $YOCl$ / YCl_3 equilibria at 1300 K. In this study, the Y/ Y_2O_3 equilibrium was employed to control the O concentration in the range of 200–2000 ppm O with varying a_Y in eutectic NaCl–KCl (l) (50 mol% NaCl–KCl). Additionally, the Y/ $YOCl$ / YCl_3 equilibrium was employed to reduce the O concentration in Ti to 30–60 ppm O in

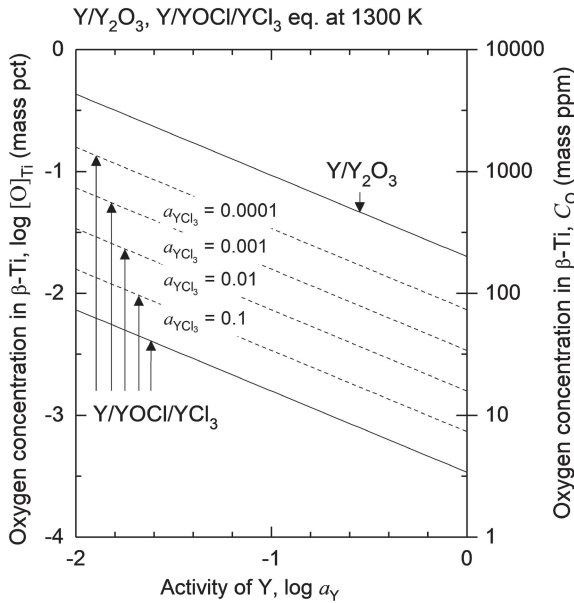


Fig. 2 Relationship between oxygen concentration in β -Ti determined by Y/Y_2O_3 and $Y/YOCl/YCl_3$ equilibria, and activity of yttrium (a_Y), varying a_{YCl_3} .^{15,54,55)}

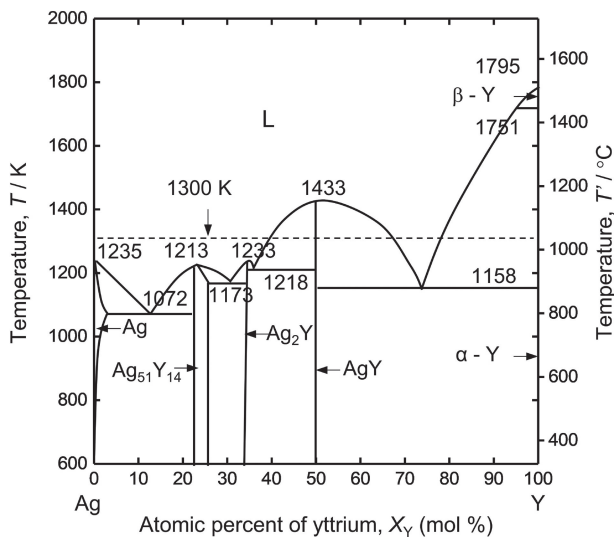


Fig. 3 Y-Ag binary phase diagram.⁵⁶⁾

$YCl_3(l)$. The difference between the calculated value (3.4 ppm O) in eq. (11) of the O concentration in Ti and the experimental value (30–60 ppm O) was caused by the inaccuracy of $\Delta G^\circ_{f,YOCl}$ and $\Delta G^\circ_{f,YCl_3}$ in the literature.⁵³⁾

To vary a_Y in the Y/Y_2O_3 equilibrium and to control p_{O_2} in the system, Y-Ag alloy was used in this study. Figure 3 shows the binary diagram of the Y-Ag system, and Fig. 4 shows the relationship between the mole fraction of Y, X_Y , in the Y-Ag alloy and a_Y at 1346 K.⁵⁷⁾ In this study, the relationship between X_Y and a_Y at 1346 K was applied as an approximation at 1300 K.

Through the thermodynamic considerations above, a new sintering process with the deoxidation of Ti using Y metal as the deoxidizing agent was designed, as shown in Fig. 5. In this process, with electron transfer in the conductive plate, O in Ti and Y dissolve into NaCl-KCl as oxide ion (O^{2-}) and yttrium ion (Y^{3+}), respectively. These ions produce Y_2O_3 (s)

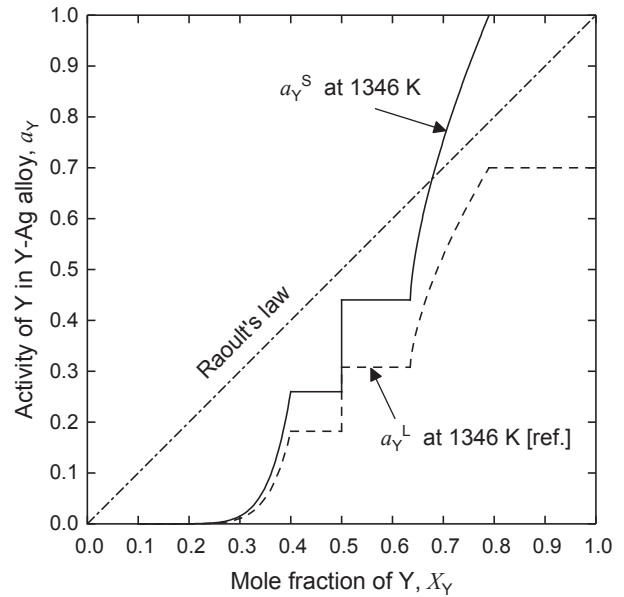


Fig. 4 Relationship between mole fraction of yttrium and activity of yttrium in Y-Ag system at 1346 K.⁵⁶⁾

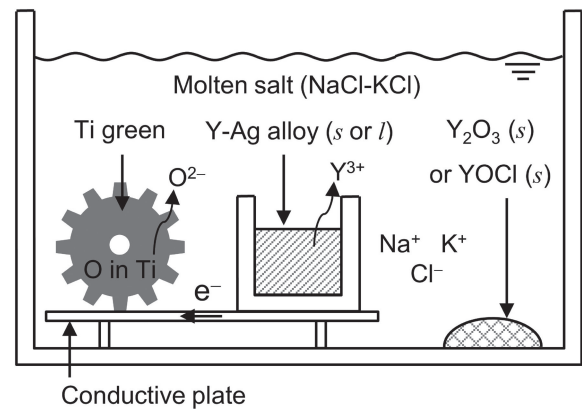


Fig. 5 Schematic illustration of the new sintering process developed in this study showing control of oxygen concentration in Ti.

or $YOCl$ (s) and the O concentration in Ti decreased following the reactions (4) and (8).

3. Experimental Procedure

Figure 6(a) shows a schematic of the experimental apparatus in a Ti crucible. Bulk Ti samples (approximately 0.1 g each) and a Ti pellet were placed in the Ti crucible, as shown in Fig. 6(a). The Ti crucibles were placed with Ti sponge (getter) in a stainless-steel container, which was completely sealed via welding. The Ti samples, which were used for measuring O concentration, were cubes having 2–3 mm sides (Ti-2B, ca. 230 ppm O), 1.2 mm diameter wires (Ti-1.2U, ca. 1200 ppm O), and 2 mm diameter wires (Ti-2L, ca. 1200 ppm O). Ti pellets were made from hydride-dehydride Ti powder (press pressure: ~ 500 MPa). Detailed information on the samples used in the experiments is shown in Table 3.

The initial amounts of samples and reagents in each lot are shown in Tables 4 and 5. In the experiments of the Y/Y_2O_3 equilibrium, approximately 1 g of Y_2O_3 was added into the

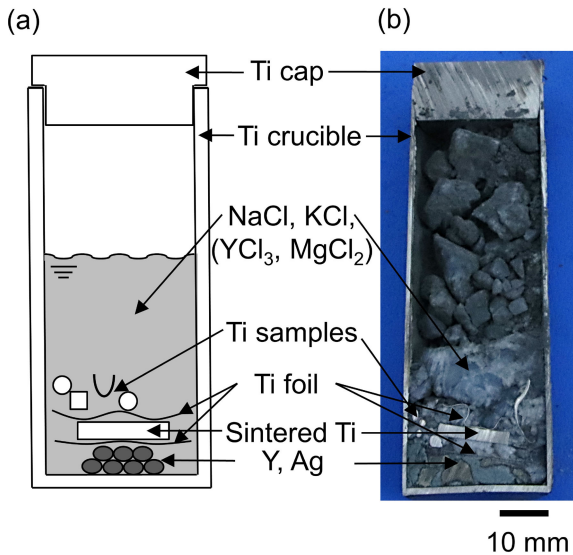


Fig. 6 (a) Schematic illustration and (b) photograph (181001-lot.3-1) of the Ti crucible.

Table 3 Materials and reagents used in the experiments.

Materials	Form	Purity / grade	Supplier / note
Ti crucible	25.4 mm in diameter 1 mm in thickness 80 mm in height	CP-Ti ^a	Shinkinzoku Industry Co., Ltd.
Ti cap		CP-Ti ^a	Shinkinzoku Industry Co., Ltd.
Ti foil	0.1 mm in thickness	CP-Ti ^a	Shinkinzoku Industry Co., Ltd.
Ti-2B	cube with 2 mm in length of side	~ 230 mass ppm O	High purity Ti sponge, electron-beam melted
Ti-1.2U	wire with 1.2 mm in diameter	~ 1200 mass ppm O	Shinkinzoku Industry Co., Ltd.
Ti-2L	wire with 2 mm in diameter	~ 1200 mass ppm O	Shinkinzoku Industry Co., Ltd.
Ti	sponge	≥ 97.0 %	Toho Titanium Co., Ltd.
Ti	HDH Powder, irregular shapes particle size: < 45 μm	≥ 99.4 % < 3500 ppm O < 300 ppm N	Osaka Titanium Technologies Co., Ltd.
Y	shot	≥ 99 %	Santoku Co., Ltd.
Ag	shot	≥ 99.99 %	Ishifuku Kinzoku Co., Ltd.
YCl ₃	powder	≥ 99.9 %, anhydrous	Alfa Aesar Co., Ltd.
Y ₂ O ₃	powder	≥ 99.9 %	Shin-Etsu Chemical Co., Ltd.
NaCl	powder	≥ 99 %	Wako Industry Co., Ltd.
KCl	powder	≥ 99 %	Wako Industry Co., Ltd.
Stainless steel crucible (tube and plate)		SUS 316, Ni: 10–14 % Cr: 16–18 % Mo: 2–3 % Fe: balanced	Azabu Industry Co., Ltd.

Caption:

a: Commercially pure titanium (≥ 99.5 %)

initial feed to maintain $a_{Y_2O_3}$ at unity. The stainless-steel container was placed in a box-type electric furnace and held at 1300 K for 173 ks. The holding time was determined based on the diffusion coefficient of O in Ti at 1300 K⁵⁸⁾ and an

Table 4 Initial amounts of samples and reagents in the Ti crucible for the experiment utilizing the Y/Y₂O₃ equilibrium.

Exp. no.	a_Y ^{a,b,c}	Initial amount of samples in the titanium crucible, m/g (n/mol)					$C_{O,theo}$ (ppm O) ^d
		NaCl	KCl	Y	Ag	Y ₂ O ₃	
181001-lot.3-1 ^e	1	16.22 (0.278)	20.68 (0.278)	4.42 (0.0497)		1.13 (0.00500)	200
181212-lot.4-1 ^e	1	14.72 (0.252)	18.78 (0.252)	5.33 (0.0599)		1.16 (0.00514)	200
181001-lot.3-2	0.44	12.86 (0.220)	16.41 (0.220)	5.33 (0.0599)	4.33 (0.0401)	1.13 (0.00500)	350
181212-lot.4-2	0.44	13.83 (0.237)	17.64 (0.237)	5.33 (0.0599)	4.32 (0.0401)	1.15 (0.00509)	350
181001-lot.3-3	0.26	14.31 (0.245)	18.26 (0.245)	4.01 (0.0451)	5.93 (0.0550)	1.13 (0.00500)	490
181212-lot.4-3	0.26	13.57 (0.232)	17.32 (0.232)	4.00 (0.0450)	5.93 (0.0550)	1.13 (0.00500)	490
181001-lot.3-4	0.09	12.09 (0.207)	15.43 (0.207)	3.11 (0.0350)	7.01 (0.0650)	1.13 (0.00500)	1000
181212-lot.4-4	0.09	16.98 (0.291)	21.66 (0.291)	3.11 (0.0350)	7.01 (0.0650)	1.13 (0.00500)	1000
181001-lot.3-5	0.03	13.20 (0.226)	16.84 (0.226)	2.22 (0.0250)	8.09 (0.0750)	1.13 (0.00500)	2000
181212-lot.4-5	0.03	16.76 (0.287)	21.39 (0.287)	2.22 (0.0250)	8.09 (0.0750)	1.13 (0.00500)	2000

Caption:

a: Activity of Y(s).

b: Calculated from the initial amount of the samples using the ref. 56.

c: As shown in Figure 5, the activity of Y in the Y–Ag system has two certain values ($a_Y = 0.44, 0.26$). Also, we set the activities for producing sintered Ti at 1000 and 2000 ppm O.

d: Theoretical deoxidation limit of Ti.

e: These values are reprinted from ref. 53.

Table 5 Initial amounts of samples and reagents in the Ti crucible for the experiment utilizing the Y/YOCl/YCl₃ eq. and the results of the oxygen concentration of Ti samples after the experiments.

Exp. no.	Initial amount of samples in the titanium crucible, m/g (n/mol)		Oxygen concentration after exp., C_O^a (ppm O)
	Y	YCl ₃	
190315-lot.6-1	2.83 (0.0318)	21.69 (0.111)	30 – 60

Caption:

a: Reported in our previous paper (ref. 53). Inert gas fusion method was used to detect oxygen (TC-600, LECO Corporation)

assumption of the time required to obtain a homogeneous distribution of O dissolved in Ti.

After holding the stainless-steel container at 1300 K, the container was quenched in water. Figure 6(b) shows a cross-section of the Ti crucible after the experiment. The Ti sample for measuring O concentration was chemically polished with a 1:4:10 mixture of HF–HNO₃–H₂O, which was sufficient to remove impurities on the surface. It was then rinsed with distilled water and alcohol before drying. The O concentrations in the Ti sample was analyzed by inert gas fusion analysis (TC-600, LECO Corporation). Detailed analysis conditions are shown in Table 6.

After the experiment, salts attached to the Ti pellet were removed using acetic acid. Then, the surface of the Ti pellet was physically polished using a buffing grinder (# 120, # 1000, and # 2000) and chemically polished with HF–

Table 6 Results of oxygen and nitrogen analyses of Ti samples in the experiment utilizing Y/Y₂O₃ equilibrium.^a

Exp. no.	a_Y^b	Types of Ti samples	Oxygen concentration, C _O (ppm O)		Analyzed error, ϵ_o (%)	C _{O,theo} (ppm O) ^c	
			Initial, C _{O,initial}	After exp., C _{O,after}			
181001-lot.3-1 ^{d,e}	1	2L ^g	1200	120	21	200	
		2B	230	120	11		
		2B	230	150	11		
181212-lot.4-1 ^{e,f}	1	2L	1200	210	11	200	
		1.2U	1200	80	23		
		2B	230	140	14		
181001-lot.3-2 ^d	0.44	2L	1200	170	22	350	
		1.2U	1200	250	30		
181212-lot.4-2 ^f	0.44	2L	1200	110	23	350	
		2L	1200	160	17		
		1.2U	1200	160	20		
		2B	230	180	21		
181001-lot.3-3 ^d	0.26	2L ^g	1200	730	5	490	
		2B	230	780	4		
181212-lot.4-3 ^f	0.26	2L	1200	700	5	490	
		1.2U	1200	500	7		
		2B	230	700	4		
181001-lot.3-4 ^d	0.09	2L	1200	1000	5	1000	
		1.2U	1200	970	4		
		2B	230	1000	4		
181212-lot.4-4 ^f	0.09	2L	1200	1200	4	1000	
		2L	1200	1200	5		
181001-lot.3-5 ^d	0.03	2L	1200	2700	3	2000	
		1.2U	1200	2300	4		
		2B	230	2500	6		
181212-lot.4-5 ^f	0.03	2L	1200	3000	3	2000	
		2L	1200	3000	3		
		1.2U	1200	1600	5		
		2B	230	1000	4		

Caption:

a: Ti samples: ~1.0 g, 2L: wire with 2 mm diameter wire, 1.2U: 1.2 mm diameter wire, 2B: cube with 2 mm side length

b: Activity of Y(s).

c: Theoretical deoxidation limit of Ti.

d: Analytical conditions:

Standard sample: steel pin ~ 1.0 g, 365±7 ppm O, part number: 501-646

Graphite crucible: ~ 1.0 g, 0.1±0.1 µg O, part number: 782-720

Ni flux: ~1.0 g, 4.4±1.9 µg O, part number: 502-344

Estimated maximum analytical error: $\epsilon_{O,max} = 30\%$,

e: These values are reprinted from ref. 53.

f: Analytical conditions:

Standard sample: steel pin ~ 1.0 g, 365±7 ppm O, part number: 501-646

Graphite crucible: ~ 1.0 g, 0.0±0.1 µg O, part number: 782-720

Ni flux: ~1.0 g, 3.4±1.5 µg O, part number: 502-344

Estimated maximum analytical error: $\epsilon_{O,max} = 23\%$

g: Two piece.

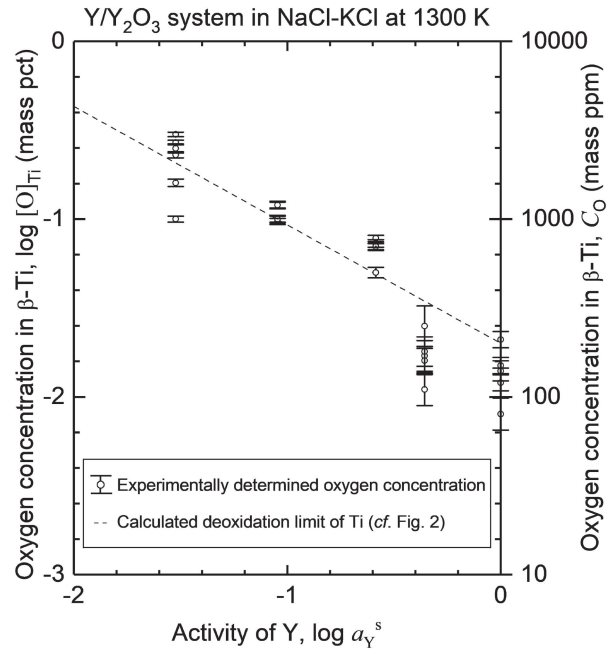
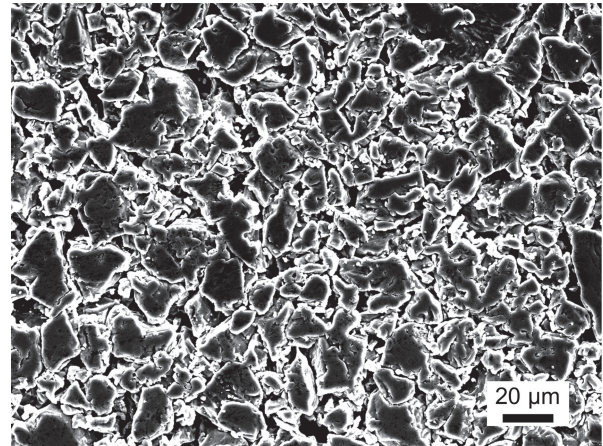
Fig. 7 The relationship between experimentally obtained oxygen concentration in the Ti samples and a_Y in Y/Y₂O₃ equilibrium.

Fig. 8 SEM image of the surface of Ti pellets in NaCl-KCl at 1300K before the experiment.

HNO₃-H₂O for approximately 30 s. Scanning electron microscopy (SEM) and energy-dispersive X-ray spectroscopy (EDS) were used to analyze the microstructure and the composition of the Ti pellet (JSM6510LV, JEOL Co., Ltd.).

4. Results and Discussions

4.1 Inert gas fusion analysis of Ti samples in the Y/Y₂O₃ equilibrium

Table 6 shows the O concentration in the Ti samples after the experiment in the Y/Y₂O₃ equilibrium. Figure 7 shows the relationship between the experimentally obtained O concentrations in Ti and a_Y in the Y-Ag alloy. As shown in Fig. 7, the results are in good agreement with calculated values using thermodynamics. These results indicate that the O concentration in Ti can be controlled reliably in the range of 200–2000 ppm O using the method designed in this study.

4.2 SEM observation and EDS mapping of Ti pellets in the Y/Y₂O₃ equilibrium and Y/YOCl/YCl₃ equilibrium

Figure 8 shows the SEM image of the surface of the Ti pellet before the experiment.

Figure 9 shows the EDS mapping of a cross-section of a Ti pellet in the experiment in the Y/Y₂O₃ equilibrium, in which pure Y metal was employed in molten NaCl-KCl (Exp. # 181001-lot.3-1). Comparison of the SEM images in Figs. 8 and 9(a) indicates that sintering of Ti powder occurred. However, as shown in Fig. 9(a), the driving force for the sintering reaction of Ti powder was not high enough to obtain a completely dense sintered body. Furthermore, Y was observed in the Ti pellet (Fig. 9(e)), which means Y contamination was occurred in the Ti pellet. In contrast, the positions of the O and chlorine (Cl) signals in the Ti pellet were unclear (Figs. 9(b), (c)). Y contamination was likely

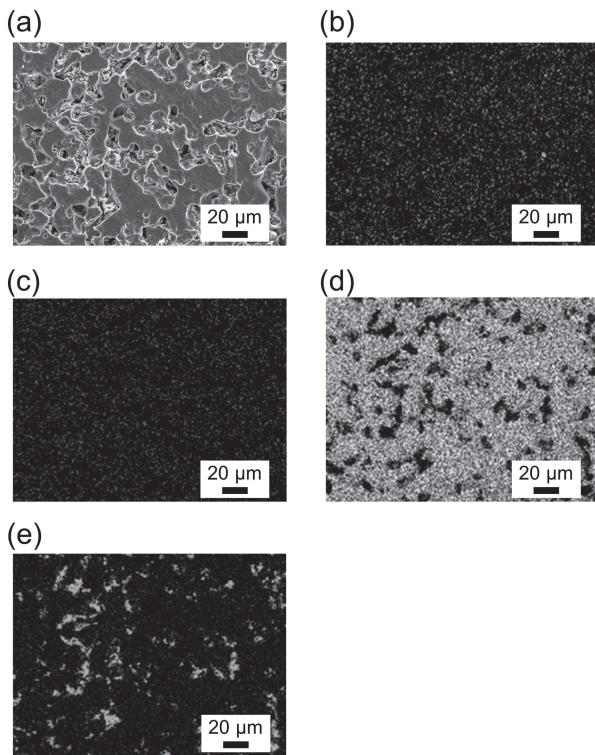


Fig. 9 EDS-mapping of the cross-section of a Ti pellet in the Y/Y₂O₃ equilibrium, after the sintering experiment (exp.181001-lot.3-1): (a) SEM image, (b) O, (c) Cl, (d) Ti, and (e) Y.

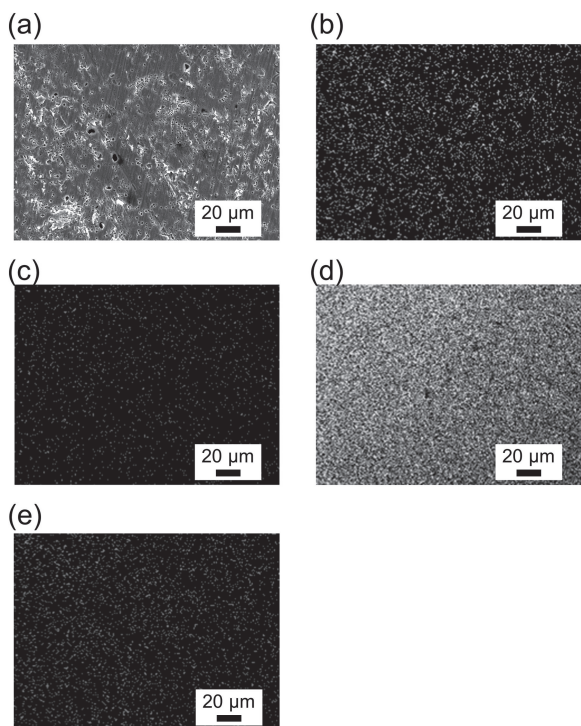


Fig. 10 EDS-mapping of the cross-section of a Ti pellet in the Y/YOCl/YCl₃ equilibrium, after the sintering experiment (exp.190315-lot.6-1): (a) SEM image, (b) O, (c) Cl, (d) Ti, and (e) Y.

caused from contact between the Ti powder and Y ions in the molten salt.

Figure 10 shows the EDS mapping of a cross-section of a Ti pellet in the Y/YOCl/YCl₃ equilibrium in YCl₃ (Exp.

#190315-lot.6-1). Figure 10 confirms that sintering occurred in this system and the sintered Ti pellet was still porous. The positions of Y, O, and Cl were not identified during the EDS mapping.

In this study, we focused mainly on thermodynamics in order to probe the deoxidation limits during the sintering process. Thus, the temperature (1300 K) was set to be lower than the general sintering temperature of PM-Ti (1500–1700 K). However, the sintering/deoxidation temperature is changeable. Higher temperatures would increase the driving force of the sintering reaction under the ultra-low p_{O_2} environment.

As mentioned, this study demonstrated that new deoxidation methods using the Y/Y₂O₃ and Y/YOCl/YCl₃ equilibria are effective to control the O concentrations in Ti, and that the sintering reaction of Ti powder proceeds in molten salt at 1300 K. However, some problems, such as contamination and porousness in the sintered Ti, remain to be solved before this deoxidation method can be applied to PM-Ti in practice. The establishment of this new process will enable the efficient fabrication of Ti products with desired low-O-concentration from low-cost high-O-concentration Ti powder.

5. Conclusion

In this study, we developed a new sintering process that could remove O from Ti using Y metal in molten salt. This study showed that the O concentration in Ti could be reliably controlled by varying the activity of Y in the Y/Y₂O₃ equilibrium in NaCl–KCl (I) and that the sintering of Ti powder co-occurred. Additionally, when the Y/YOCl/YCl₃ equilibrium was employed to reduce the O concentration in Ti to 30–60 ppm O in YCl₃ (I), the sintering of Ti powder also proceeded. This study demonstrated the possibility of the development of a new sintering process, in which the O concentration of Ti can be controlled to 30–2000 ppm O.

Acknowledgments

We are grateful to Dr. Lingxin Kong and Mr. Takara Tanaka at The University of Tokyo for their helpful suggestions and help with the experiments. This work was financially supported by the Japan Society for the Promotion of Science (JSPS) through a Grant-in-Aid for Scientific Research (S) (KAKENHI Grant No. 26220910, and 19H05623).

REFERENCES

- 1) M.F. Ashby: *Materials Selection in Mechanical Design*, third ed., (Butterworth-Heinemann, Burlington, U.S., 2005).
- 2) M. Niinomi: *Mater. Sci. Eng. A* **243** (1998) 231–236.
- 3) The Japan Titanium Society: *Titan (Gemba De Ikasu Kinzoku Zairyo Series)* in Japanese, (Maruzen, Tokyo, Japan, 2011).
- 4) B.H. Kasemo: *J. Prosthet. Dent.* **49** (1983) 832–837.
- 5) K.K. Turekian and K.H. Wedepohl: *Geol. Soc. Am. Bull.* **72** (1961) 175–192.
- 6) U.S. Department of the Interior and U.S. Geological Survey, Mineral Commodity Summaries 2019. <https://www.usgs.gov/centers/nmic/mineral-commodity-summaries/>, 2019 (accessed on 6 January 2020).
- 7) O. Takeda and T.H. Okabe: *JOM* **71** (2019) 1981–1990.

- 8) M. Yamaguchi, M. Yamaguchi and R.O. Suzuki: *Titanium Japan* **54** (2006) 78–82 (in Japanese).
- 9) D.J. Fray: *Int. Mater. Rev.* **53** (2008) 317–325.
- 10) Z.Z. Fang, J.D. Paramore, P. Sun, K.S.R. Chandran, Y. Zhang, Y. Xia, F. Cao, M. Koopman and M. Free: *Int. Mater. Rev.* **63** (2018) 407–459.
- 11) P.C. Rath: *SGAT Bulletin* **17** (2016) 10–23.
- 12) Y. Ito: doctoral thesis in Kyushu University, (2015, in Japanese).
- 13) R.I. Jaffee, H.R. Ogden and D.J. Maykuth: *JOM* **2** (1950) 1261–1266.
- 14) H.R. Ogden and R.I. Jaffee: *Titanium Metallurgical Laboratory Report*, (Battelle Memorial Institute, Ohio, U.S., 1955) Vol. 20.
- 15) T.H. Okabe, T. Oishi and K. Ono: *J. Alloy. Compd.* **184** (1992) 43–56.
- 16) M. Yan, W. Xu, M.S. Dargusch, H.P. Tang, M. Brandt and M. Qian: *Powder Metall.* **57** (2014) 251–257.
- 17) L. Lefebvre, E. Baril and L. Camaret: *J. Mater. Res.* **28** (2013) 2453–2460.
- 18) L. Grainger: Additive World Conference II, March 27th 2014, <https://additiveworld.com/Conferences/Additive-world-conference-2014> (accessed on 6 January 2020).
- 19) Powder Metallurgy Review, MetalYSIS' titanium powder used to 3D print automotive parts, <https://www.pm-review.com/metalysis-titanium-powder-used-to-3d-print-automotive-parts/> (accessed on 6 January 2020).
- 20) S. Abkowitz, J.M. Siergiej and R.D. Regan: *Parts and Composites, Modern Developments in Powder Metallurgy*, (Metal Powder Industries Federation, Princeton, NJ, 1971) Vol. 4, pp. 501–511.
- 21) K. Majima, T. Isono and K. Shoji: *J. Jpn. Soc. Powder Metall.* **33** (1986) 28–33 (in Japanese).
- 22) P.K. Tripathy, M. Gauthier and D.J. Fray: *Metall. Mater. Trans. B* **38** (2007) 893–900.
- 23) L. Strezov, I. Ratchev, S. Osborn and K. Mukunthan: US Patent No. 7156974 B2, (2007).
- 24) J.-C. Choi, S.-H. Chang, Y.-H. Cha and I.-H. Oh: *Korean J. Mater. Res.* **19** (2009) 397–402.
- 25) A.T. Sidambe, I.A. Figueroa, H.G.C. Hamilton and I. Todda: *J. Mater. Process. Technol.* **212** (2012) 1591–1597.
- 26) S.D. Luo, C.L. Guan, Y.F. Yang, G.B. Schaffer and M. Qian: *Metall. Mater. Trans. A* **44** (2013) 1842–1851.
- 27) E. Carreño-Morelli, J.-E. Bidaux, M. Rodríguez-Arbaizar, H. Girard and H. Hamdan: *Powder Metall.* **57** (2014) 89–92.
- 28) J.M. Oh, I.H. Choi, C.Y. Suh, H. Kwon, J.W. Lim and K.M. Roh: *Met. Mater. Int.* **22** (2016) 488–492.
- 29) Z.Z. Fang, P. Sun, Y. Xia and Y. Zhang: US Patent No. 2017/0113273 A1, (2017).
- 30) D. Hu and G.Z. Chen: *ECS Trans.* **50** (2013) 29–37.
- 31) D. Hu, A. Dolganov, M. Ma, B. Bhattacharya, M.T. Bishop and G.Z. Chen: *JOM* **70** (2018) 129–137.
- 32) T. Maetani, T. Maetani, J. Ota and H. Suzuki: Japan Patent, JPH0790318A, (1993).
- 33) T.-W. Na, W.R. Kim, S.-M. Yang, O. Kwon, J.M. Park, G.-H. Kim, K.-H. Jung, C.-W. Lee, H.-K. Park and H.G. Kim: *Mater. Charact.* **143** (2018) 110–117.
- 34) H.-K. Park, T.-W. Na, S.-M. Yang, G.-H. Kim, B.-S. Lee and H.G. Kim: *Mater. Lett.* **236** (2019) 106–108.
- 35) T.H. Okabe, R.O. Suzuki, T. Oishi and K. Ono: *Mater. Trans. JIM* **32** (1991) 485–488.
- 36) J.-M. Oh, B.-K. Lee, C.-Y. Suh, S.-W. Cho and J.-W. Lim: *Powder Metall.* **55** (2012) 402–404.
- 37) J.W. Lim, J.M. Oh, B.K. Lee, C.Y. Suh and S.W. Cho: US Patent No. 8,449,813, (2013).
- 38) J.W. Lim, J.M. Oh, B.K. Lee, C.Y. Suh and S.W. Cho: US Patent No. 8,449,646, (2013).
- 39) J.-M. Oh, H. Kwon, W. Kim and J.-W. Lim: *Thin Solid Films* **551** (2014) 98–101.
- 40) J.-M. Oh, C.-Y. Suh, H. Kwon, J.-W. Lim and K.-M. Roh: *J. Korean Inst. Resour. Recycling* **24** (2015) 21–27 (in Korean).
- 41) S.-J. Kim, J.-M. Oh and J.-W. Lim: *Met. Mater. Int.* **22** (2016) 658–662.
- 42) C.-I. Hong, J.-M. Oh, J. Park, J.-M. Yoon and J.-W. Lim: *Adv. Powder Technol.* **29** (2018) 1640–1643.
- 43) J.-M. Oh, C.-I. Hong and J.-W. Lim: *Adv. Powder Metall.* **30** (2019) 1–5.
- 44) G.Z. Chen, D.J. Fray and T.W. Farthing: *Nature* **407** (2000) 361–364.
- 45) Roskill Information Services, Rare Earths: *Global Industry, Markets and Outlook to 2026*, 16th ed., (London, U.K., 2016).
- 46) M. Yang, H.P. Tang and M. Qian: *Titanium Powder Metallurgy*, (Elsevier, Waltham, U.S., 2015) pp. 253–276.
- 47) Y.F. Yang, S.F. Li, M. Qian, Q.S. Zhu, C.Q. Hu and Y. Shi: *J. Alloy. Compd.* **764** (2018) 467–475.
- 48) B. Poorganji, A. Kazahari, T. Narushima, C. Ouchi and T. Furuhashi: *J. Phys. Conf. Ser.* **240** (2010) 012170.
- 49) T.H. Okabe, T. Deura, T. Oishi, K. Ono and D.R. Sadoway: *J. Alloy. Compd.* **237** (1996) 150–154.
- 50) T.H. Okabe, T. Deura, T. Oishi, K. Ono and D.R. Sadoway: *Metall. Trans. B* **27** (1996) 841–847.
- 51) T.H. Okabe, K. Hirota, E. Kasai, F. Saito, Y. Waseda and K.T. Jacob: *J. Alloy. Compd.* **279** (1998) 184–191.
- 52) T.H. Okabe, K. Hirota, Y. Waseda and K.T. Jacob: *J. MMIJ* **114** (1998) 813–818.
- 53) A. Iizuka, T. Ouchi and T.H. Okabe: *Metall. Mater. Trans. B*, in press. doi:10.1007/s11663-019-01742-6 (accessed on 6 January 2020).
- 54) I. Barin: *Thermochemical Data of Pure Substances*, third ed., (VCH Verlagsgesellschaft mbH, Weinheim, Germany, 1995).
- 55) Y.B. Patrikeev, G.I. Novikov and V.V. Badovskii: *Russ. J. Phys. Chem.* **47** (1973) 284.
- 56) C.E. Lundin and D.T. Klodt: *Trans. Met. Soc. AIME* **224** (1962) 367–372.
- 57) O. Madelung: *Landolt-Börnstein - Group IV Physical Chemistry book series*, (Berlin, Germany, 1991).
- 58) C.J. Rosa: *Metall. Trans.* **1** (1970) 2517–2522.